Energy Harvesting Nanostructured Porous Silicon Scaffolds for Enhanced Efficiency Biofuel Cells

Mohamad Hajj-Hassan, Hussein Hajj-Hassan, Hassan M. Khachfe
Dept. of Biomedical Engineering
Lebanese International University
Beirut, Lebanon
mohamad.hajjhassan@liu.edu.lb, houssein.hajjhassan@liu.edu.lb, hassan.khachfe@liu.edu.lb

***Abstract*— An Enzymatic biofuel cell is a specific type of fuel cell which uses enzymes as catalysts to oxidize its fuel. Because of their efficient size and immobility, they pose as a great promise in terms of their relatively inexpensive components and fuels, as well as a potential power source for bionic implants. Here, we present the use of dry-etched nanotextured porous silicon scaffolds as a basis for new biofuel designs. Such an architecture increases the contact surface area of silicon with surrounding biofuel to enhance the process of harvesting of energy, and consequently, the efficiency of the cell.**

Keywords-nanotechnology; porous silicon; biofuel cell

I. INTRODUCTION

Recent advances in micro and nanotechnologies allow the development of implantable, portable, and miniature devices for a broad range of applications, including biomedical fields [1]. Powering implantable medical devices necessitates the development of lightweight, non-toxic and stable sources of energy with long life spans. In fact, the number of battery charging cycles in micro-energy harvesting methods is a major source of limitation [2]. Several micro-energy harvesting sources have been already identified in previous research, namely, low and high frequency electromagnetic Radio Frequency (RF) signal harvesting, conversion of vibration into energy, thermal and pressure gradients energy harvesting in addition to the latest attempts towards organic energy generation directly within the human body using fuel cells [3, 4].

Harvesting energy using ambient vibration has been the focus of various projects [5-7]. Devices made for this purpose are mechanically modeled with a base excitation of an elastically mounted seismic mass moving past a coil. Optimal architecture for maximal power generation under different operating conditions has also been shown [8]. Various applications of this principle have manifested in systems integrated in footwear to harvest energy from walking [9], while in other designs piezoelectric and electromagnetic generators convert pressure variations into electricity [10]. The power generated using these methods ranges from tens to hundreds of milliwatts [4, 7, 8]. On the other hand, several studies have focused on energy harvesting from low frequency vibrations [7, 11]. This concept was made viable by creating a generator that converts low-frequency environmental vibrations to a higher frequency by employing the frequency up conversion technique [12, 13]. One major limitation of this technology is encountered with patients that are not able to perform any physical activities in order to power the generator and, hence, produce the necessary charging current.

Energy harvesting using RF inductive coupling is a very promising technology, particularly in the presence of such a wide variety of RF signals in our everyday environment. Additionally, this technology can also be used to send data back to a base station, thus creating a two-way link. The system consists of a power generating circuit linked to a receiving antenna in order to capture the RF signal and convert it to a DC voltage [14]. The main challenge in this technology is in the receiver's capacity to read various frequencies, as well as the use of efficient power rectifiers. Several interesting studies have reported either the use of multiple energy harvesting antennas in one area [15], which has shown that an increase of 83% in area results in 300% increase in power, or the design of a high efficiency, ultra-low voltage active rectifiers [16].

This article covers the use of porous silicon scaffolds for biofuel cells. The next section presents and compares different types of biofuel cells. Section III introduces the immobilization and electrodes configurations for energy harvesting. Section IV presents porous silicon technology. Section V discusses existing porous silicon fabrication techniques. Section IV details the fabrication process of the porous silicon scaffolds using XeF_2.

II. BIOFUEL CELLS

The first enzyme based glucose/O_2 fuel cell to generate electricity was introduced in 1964 by Yahiro et al., aiming at using this concept to power an artificial heart [17]. While the field of fuel cell research has flourished in various industrial and environmental arenas, biomedical applications started making use of the technology only after 2001, with recent successes in micro fuel cell technology [18-20]. The two most dominant classifications of fuel cells are enzymatic, illustrated in Fig. 1, and microbial, based on the catalyst used to oxidize or reduce the fuel used in the design [21]. While microbial catalysts offer more longevity to the fuel cell, microbial fuel cells require a barrier between the cathode and the anode and between the fuel cell and its surrounding

environment [22]. Such a design increases its size and decreases the current density since the fuel cell lacks direct contact with the fuel. Most importantly, when it comes to the use of microbial fuel cell for implantable devices, long term infections, thrombosis and other types of complications raise serious concerns [23, 24]. Therefore, it is natural that the use of microbial fuel cells was limited to few studies, one of them suggesting its use within the intestinal environment inside the transverse colon [25]. On the other hand, enzymatic fuel cells have lower stability and shorter lifespan because the longevity of enzymes is in the range of 10 days [26]. This has driven research in enzymatic fuel cells towards short term uses such as glucose sensors, post-op temperature measurement or as a power supply for pressure sensors indicating blockage of fluid flow in the nervous system [23]. However, since enzymes are selective in nature, the design of enzymatic fuel cells can be made into microscopic sizes without the need for a separating membrane to regulate the flow of the fluid and enzymes used in its design, thus achieving higher power densities due to the direct contact between the probes and the fuel [26]. Continuous attempts to increase the lifetime of the enzymes exist using immobilization techniques or using magnetic iron nanoparticles that shield the enzymes from getting oxidized or self-digested [27].

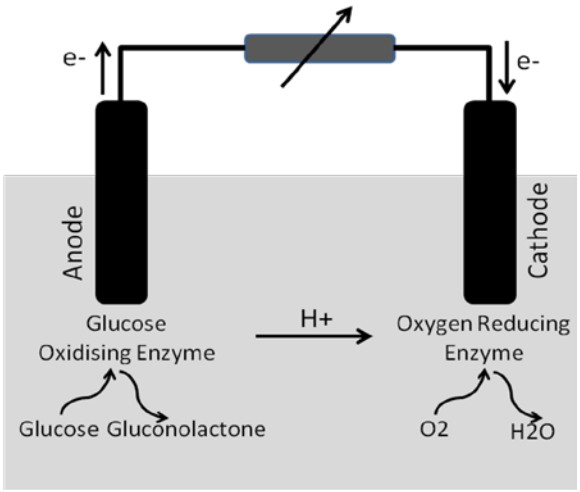

Figure 1. Illustration of an enzymatic biofuel cell using Glucose and Oxygen.

Another important factor in the design of the fuel cell is the target fuel. Although most implantable fuel cell studies have focused so far on the use of blood stream glucose, some studies have considered other alternatives such as the use of white blood cells based on their ability to generate electron current across their cellular membrane [28-30].

Most importantly, the complex environment inside the human body, such as the amount of glucose and oxygen available in addition to the neo-vascular build up that can hinder the exposure of the fuel cell to body fluids, represent important obstacles that any fuel cell design have to overcome in order for it to become a viable one [29]. Based on the first in-vivo study conducted by Cinquin et al., an enzymatic fuel cell was built by adjusting the types of enzymes used in order to account for the specific PH, concentration, and the effect of urea presence on the fuel cell [31]. This was implanted inside the peritoneal cavity of a rat, and has proven to provide a stable power of more than 7.52 μW/mL for a period of three months [31].

Here, we are interested in increasing the efficiency of energy harvesting in enzymatic fuel cells by increasing the contact surface area between the harvesting probes and the surrounding fuel. This can be achieved by (1) using porous interface to provide a large surface to volume ratio and consequently lager area of contact with enzymes (2) increasing the area of electrodes collecting the resulting amount electrons by using an array of electrodes. Doped porous silicon represents a good candidate due to the fact that it combines both biocompatibility and electrical conductivity [32, 33].

III. IMMOBILIZATIONS AND ELECTRODES PLATFORM

The proper functioning of an enzyme-based biofuel cell relies on both the chemical and physical properties of the immobilized enzyme layer. Physical and chemical methods can be used for immobilization of enzymes. Physical methods include: (1) Gel entrapment wherein enzymes are entrapped in a gel matrix, such as gelatine and polyacrylamide, as well as dialysis tubing [34]. (2) Adsorption where no additional reagents are required but only weak bonding involved between enzymes and electrode surface. Chemical methods are the main methods used for developing enzyme-based biofuel cells. The methods include covalent immobilization and immobilizing enzyme in polymer matrix.

Although enzymes are highly efficient catalysts they are difficult to incorporate into fuel cells. Low catalytic efficiency and stability of enzymes have been seen as barriers for the development of large-scale operations to compete with traditional chemical processes. This can be tackled with the use of nanostructured materials possessing large surface areas leading usually to high enzyme loading, resulting in improvement of power density of the biofuel cells.

Fig. 2 is the schematic representation of the novel enhanced porous silicon biofuel cell. It consists of an array of inter-digitized fingers made out of silicon covered by a layer of gold. The area between the inter-digitized fingers is made porous for entrapping and better immobilization of enzymes. The energy harvesting process is based on oxidation-reduction reactions taking place between the two arrays of inter-digitized fingers so that one array can be the anode and the second array can be cathode. Using microfabrication technology, it is possible to obtain identical anode and cathode electrodes. The enzymes get attached and immobilized between the two electrodes which in turn collect the resulting electrons and relay them to electronic circuit.

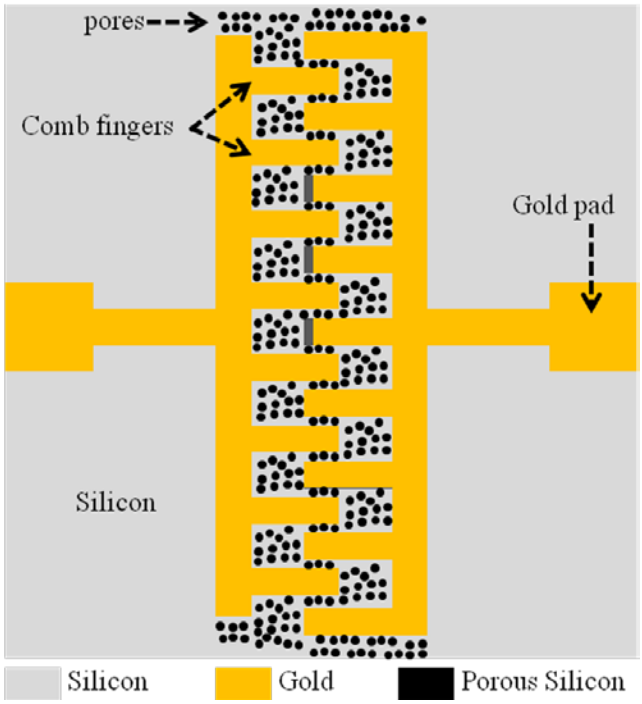

Figure 2. Schematic representation of the enhanced enzymatic biofuel cell.

IV. POROUS SILCION TECHNOLOGY

Implantable biomedical devices built from bulk silicon have been available for biosensing and actuating applications for several years. However, this form of silicon is not biocompatible and so far this has prevented its use in vivo. Bulk silicon-based devices need coating or packaging in a biocompatible material, if they are to be used in and linked to living tissues [32, 33]. The majority of today's medical devices are coated with materials such as Polyvinylchloride (PVC), polypropylene, polycarbonate, fluorinated plastics and stainless steel. These materials are tolerated by the human body and are described as bioinert. An effective biomaterial, however, must bond to living tissue and is known as bioactive.

Nanostructured porous silicon (PS), whose particular texture can be described as a network of pores interconnected by solid nanocrystalline silicon, has properties that make it a very promising bioactive biomaterial [35, 36], in particular for devices that need to be linked to the biological system such as implantable devices [37]. Porous silicon material is useful and attractive for a wide variety of applications to develop biological sensors [37-39] and biomedical devices [40, 41]. This has significantly increased the interest in using porous silicon in biofuel cells.

An essential requirement for fabricating porous silicon in different applications is to have the ability to vary the size and configuration of the pores by choosing the appropriate fabrication parameters and conditions. For instance, for photonic bandgap filters, the pores are designed to the on the order of the wavelength of the light to retain and tune the optical reflectivity of the porous silicon [42, 43]. For biological sample filters, the pore size has to be large enough to allow the desired biomolecules to be filtered and cross through the pores freely [44].

V. FABRICATION OF POROUS SILCON

Many previous reports have shown that porous silicon can be prepared through a galvanostatic, chemical, or photochemical etching procedures in the presence of hydrofluoric (HF) acid solutions or through stain etching [45-47]. Other methods such as pulsed anodic etching [48] and magnetic-field assisted anodization [49] were also employed for porous silicon preparation. In these techniques, the pore characteristics such as diameter, geometric shape and direction of the pores not only depend on the composition of the etching solution, but they also depend on temperature, current density, crystal orientation, dopant and doping density of the silicon substrate [45, 47, 50]. Moreover, porous silicon produced on large surface areas along with high porosity and/or thickness leads to a systematic cracking of the layer during the evaporation of the etching solvent. The origin of the cracking is the large capillary stress associated with evaporation from the pores. During the evaporation process, a pressure drop occurs across the gas/liquid interface that forms inside the pores [51].

A. Gas-Based Etching Technique

Gas etching method provides a suitable solution for the usage of the wet etching methods [52]. Due to the use conventional integrated circuit technology, the wet etching methods are not compatible with the widespread use of gas cluster tools. Moreover, wet etching techniques generate large quantities of dangerous waste in the manufacturing environment.

A mixture of oxygen (O_2) and nitrogen dioxide (NO_2) gases are combined with hydrogen fluoride (HF) and water vapors to produce photo-luminescent porous silicon layers as depicted in Fig. 3. The processes that were taken into account in the selection of these gases could be represented by a combination of the following chemical reactions.

Formation of nitric acid:

$$4NO_2 + 2H_2O + O_2 \rightarrow HNO_3$$
$$2NO_2 + H_2O \rightarrow HNO_2 + HNO_3$$
$$3HNO_2 \rightarrow HNO_3 + 2NO + H_2O$$
$$2NO + O_2 \rightarrow 2NO_2$$

Oxidation of silicon:

$$4HNO_3 + Si \rightarrow SiO_2 + 2H_2O + 4NO_2$$
$$Si + O_2 \rightarrow SiO_2$$

Etching of silicon dioxide:

$$SiO_2 + 6HF \rightarrow H_2SiF_6 + 2H_2O$$

The gas etching technique consists of exposing silicon samples to a mixture of O_2 and NO_2 gases in addition to HF and water vapors.

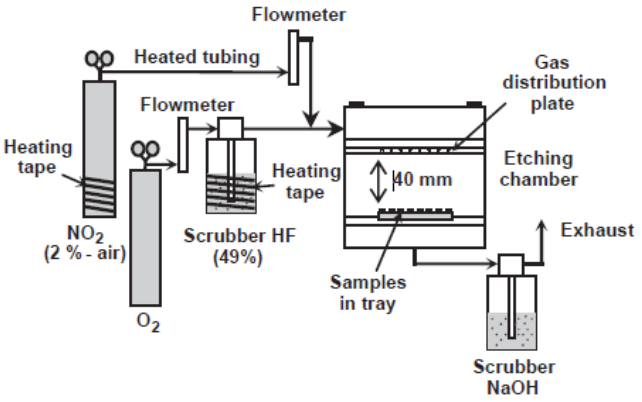

Figure 3. Schematic of the gas etching setup[52].

The experimental details were listed as follow:

- Silicon samples were loaded onto a tray that was mounted at the bottom of a chamber.
- The chamber was sealed after installing a gas distribution plate which aims to improve the uniformity of the gas flow. Noted that the chamber, tray, and distribution plate were made of chemically inert Teflon.
- Pure oxygen (99.995%) was flown through a scrubber containing HF (47-51%). The HF chamber could be kept at room temperature or heated up to 70℃.
- The scrubber HF merges with a flow of diluted nitrogen dioxide (2%) before entering the etching chamber. The NO_2 cylinder was heated at its base to a temperature of 40℃ to avoid accumulation of nitrogen dioxide at its bottom and enhance the mixing of NO_2 and air.
- The stainless steel tubing connection the NO_2 cylinder to the chamber was heated to a temperature of 30℃ to avoid the condensation of NO_2 on the tubing wall.
- The outlet of the chamber is connected to a scrubber containing sodium hydroxide (NaOH) solution which neutralizes the HF.
- The flow rates of O_2 and NO_2 could be varied by a flow-meter. The flow of O_2 and NO_2 varied between 10-50 ml/min.
- Samples are rinsed using ethyl alcohol (95%)
- Substrates are dipped in ethyl alcohol for 5 minutes and then removed.
- Substrates are left to dry in a high purity nitrogen environment (99.95%).
- Silicon samples were obtained from the dicing of boron-doped p-type wafers whose electrical resistivity was 20Ω.
- Samples were cleaned using RCA-type hydrogen peroxide mixtures, etched in a 5% HF solution for 2 minutes, rinsed in deionized water for 5 minutes, and then oxidized at room temperature in a SLM flow rate of ozone (O_3) gas with the presence of nitrogen for 5 minutes.
- Note that is cleaning sequence allowed a stringent control of the sample surface, yielding a hydrophilic surface.
- At the end of oxidization step, samples were loaded in the chamber and etching was performed for a time of 30 minutes.
- The morphology of the porous layers was investigated by a scanning electron microscopy. And the photo-luminescence properties of the porous layers were investigated using a photo-detection system (Fluorescence, PDS).

B. Stain Etching Technique

The formation of porous silicon by the strain etching process was conducted on p-type and n-type silicon wafers having different doping concentrations. Different porosity gradients were conducted since strain etching is a wet etching method which attacks the pore wall.

Experimental Procedure:

- Porous silicon layers were prepared on p-type and n-type wafers with doping concentrations of 2 x 10^{15} atom/cm³.
- More layers were prepared on p+ type and n+ type with doping concentration of 5 x 10^{18} atom/cm³
- Noted that the doping materials could be boron or phosphorus.
- The solutions for strain etching contained concentrated hydrofluoric acid and nitric acid with ratios between 50:1 and 500:1 [53, 54].
- Two additives were added into the solution, sodium-nitrite with a concentration of between 0.1 and 0.6 g/l in order to reduce the incubation time on PSL formation [55] and a surface-active substance to ensure that the evolving bubbles do not stick to the silicon surface [56].
- The mass of dissolved Si was 1 x 10^{-4} g.
- The as-grown porous layer was characterized by spectroscopic ellipsometrical(SE) measurements at 75° nominal angle of incidence in the spectral range from 280 to 840 nm.

By means of the gravimetrical and the spectroscopic ellipsometrical measurements the formation process of stain-etched PSL reveals continuous dissolution of the top surface of the layer and simultaneous formation of porous Si at the porous-crystalline interface. As a result, the stain-etched PSLs have self-limiting thickness when n-type substrates or low doped p-type substrates are used. The structural and optical characterization proved the existence of a porosity gradient in the layers, which stems from the partial dissolution of the pore walls and the top surface during formation. The morphology of the final structure is characterized by a random pore propagation direction in the case of low doped p-type and low and highly doped n-type silicon.

C. Electro-Chemical Etching Technique [11]

Electro-chemical etching is simply presented by the 'AMMT Porous Silicon Fabrication System'. This system is specifically designed for the fabrication of porous silicon using hydrofluoric acid as illustrated in Fig. 4. The user must wear appreciate safety gear and follow the safety guidelines set by the UCLA (University of California, Los Angeles) Nanolab using Hydrofluoric Acid.

The system contains:

1. Porous Silicon Bath (PSB): two chamber of HF-bath for porous silicon formation which are electrically isolated.
2. Waste Jug: located at the lower level of the PSB and is connected to the two HF drain valves.
3. Water Holders: two different water holders are available, one for the wafer and the other for the small samples.
4. Power Supply (Galvanostat): provide up to 24 A of electrical current.
5. Porous Silicon Galvanostat Software: Installed on the computer and enables the user to set the parameters and time etching.
6. Light source: 20 Watt halogen lamp located in front of the illumination windows.

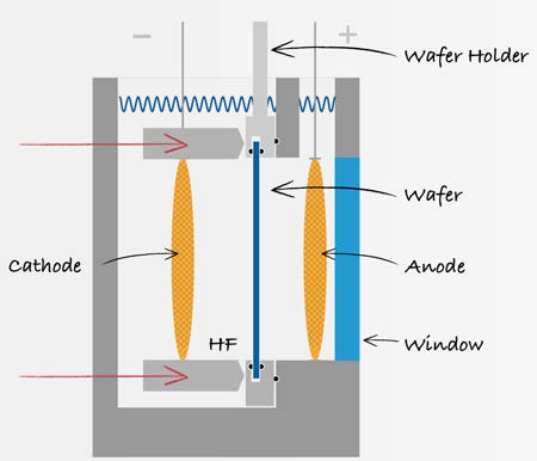

Figure 4. Schematic schematically setup of anodic experiment.

Preparation Process:

1. Cleaning: water should be cleaned from any impurities to ensure optimal porous etching result.
2. HF Preparation: wear the complete safety gear and check the drain valves.
3. Sample Mounting: mount the wafer in one of the wafer holders and place the wafer into the gap between the bayonet and the separator plate.
4. Electrode Positioning: place the electrodes in position with respect to the mounted wafer.

Noted that the electric contact of the electrode and the wafer is made through the HF electrolyte where no physical contact is required.

Fabrication Process:

1. Connect the PSB to the power supply.
2. Open the software and set the etching parameter.
3. To ensure illumination during etching, place the lamp close to the side window.
4. Set the timer for the desired time of etching.
5. After etching is over, turn off the power supply.

D. Photo-Chemical Etching Technique

The anodization is an easy method by which to form a luminescence layer on single crystalline Si. There are many difficulties in forming porous silicon on silicon on insulator (SOI) structure or on multilayered integrated circuit, since the anodization method requires electrodes in electrolyte solutions and on the back surface of a Si wafer. This becomes an obstacle for the applications of the PS for visible luminescence layers. A photochemical etching method that requires no electrode to form a visible luminescence layer on a single crystalline Si wafer is studied [57, 58].

Fig. 5 illustrates the following experimental procedure:

- An n-type (0.22-0.38 and 35-45 Ohm-cm) silicon wafer (100) was set at the bottom of the vessel filled with an etchant.
- A mixture of hydrogen fluoride acid solution (HF) and hydrogen peroxide (H 2O 2) as an oxidant were used for the etchant.
- Noted that the etchant concentration varied with HF: H_2O_2 = 100:17 ~ 250 for volume ratio.
- The silicon wafer surface was irradiated by a He-Ne laser (633 nm, 18.4 mW /cm²) as a visible laser for 5-45 minutes in order to form photochemically etched silicon.

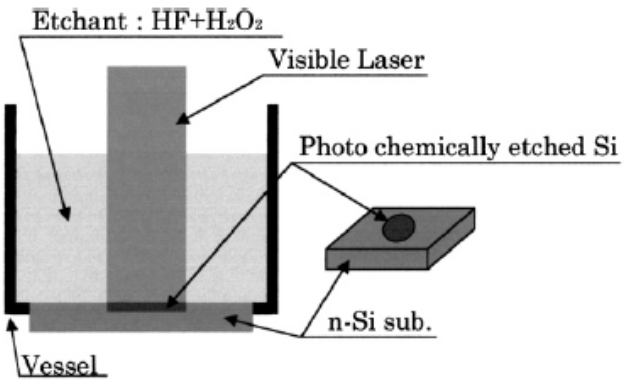

Figure 5. Schematic set up for a photochemical etching method [59].

The following reaction model of photochemical etching process of silicon atoms is depicted in Fig.6.

- He-Ne laser irradiation forms an electron-hole pair as a carrier in the Si substrate.
- H_2O molecular attacks to the wafer surface.
- Silicon atom is oxidized by H_2O and holes.

$Si + 2H_2O + nh^+ \rightarrow SiO_2 + 4H^+ + (4 - n)e^-$

h^+: hole, e^-: electron, $n \leq 4$

1. The SiO_2 region is solved by HF; therefore this means that a silicon atom is etched from the wafer.
2. H_2O_2 as an oxidant removes electrons left in the substrate, and H_2O_2 molecular and H^+ ions change into water molecules.

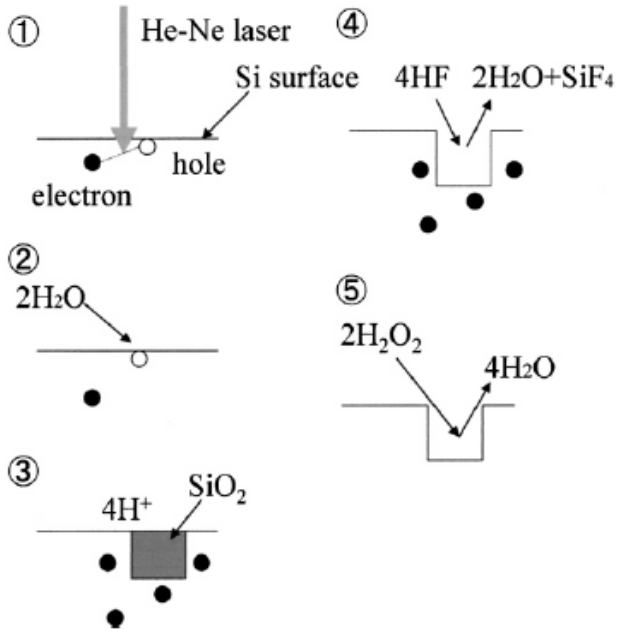

Figure 6. Schematic chemical reaction model of photochemical etching process of silicon atoms [58].

E. Chemical-Based Fabrication Technique

Porous silicon is usually fabricated under anodic polarization in an electrochemical cell. Another technique is introduced to form porous silicon without the use of any external source. Etching will occur by the formation of a galvanic cell, with the silicon acting as local anode and the metal as local cathode [60].

Experimental Procedures

1. Use of <100>-oriented n-type or p-type silicon with a resistivity of 2-5 Ω cm.
2. Etching of the sample with a dilute of HF solution with the use of some ethanol to prevent the formation of hydrogen bubbles.
3. Oxygen is the solution served as an oxidizing agent for the galvanic cell.
4. H_2O_2 may be added to increase the concentration of the oxidizing agent knowing that these agents are not reduced at the p-type silicon and do not cause the semiconductor to be etched chemically.

Two types of experiments could be performed.

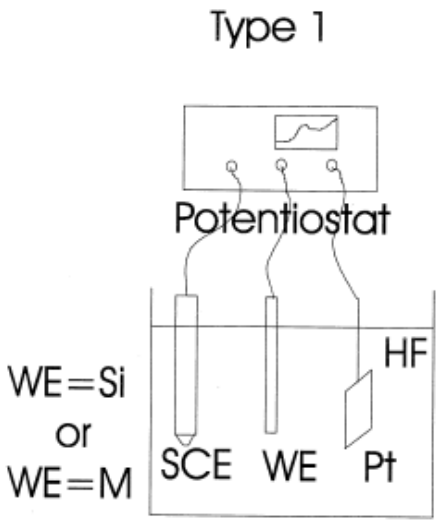

Figure 7. Schematic set up of type 1 experiment [60].

The experiments of type 1, illustrated in Fig. 7, were performed with either a Si working electrode (WE) or a metal (M) WE. A potentiostat the potential of the working electrode was regulated with respect to a standard calomel electrode (SCE). The current was measured between the WE and the Point counter electrode (Pt).

1. POS703 Bank potentiostat resulted in the formation of the current-potential curves of silicon and metal electrodes in HF solution (scan rate of 1mv /s).
2. The potential is always cited with respect to the standard calomel electrode (SCE) and the current is measured between a working electrode (WE) and a Point counter electrode (Pt).
3. The area of the silicon electrode was 0.5 cm^2 and the edges were protected from the solution by a HF resistant O-ring.
4. The galvanic cell formation is obtained when the Si electrode is connected in short circuit to the metal electrode.

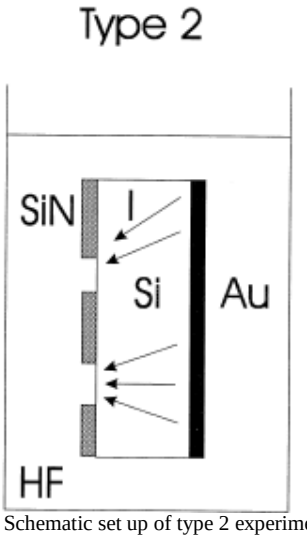

Figure 8. Schematic set up of type 2 experiment [60].

Experiments of type 2, illustrated in Fig. 8, were performed with an Au electrode on chip, noted that the potentials or currents could not be measured. This experiment demonstrates the formation of porous silicon without external contacts.

- A silicon nitride etch mask was deposited on one side of the wafer.
- An inert metal electrode was formed on the other side of the wafer by evaporation a film of Au /Cu.
- The metal /exposed silicon are ratio was typically 16.

The main advantage of galvanic porous formation technique is that a special sample holder to contact the Si is not required. This makes the technique suitable for batch fabrication of porous silicon devices. The contact between the silicon sample and a layer of noble metal is mandatory. The etching rate may be controlled by the metal /Si area ration and the concentration of oxidizing agent in solution.

F. Pulsed Current Etching

This technique for porous silicon formation is based on pulsed current anodic etching. The technique offers the possibility of fabricating luminescence material with selective wavelength emission depending on cycle time (T) and pause time (Toff) of pulsed current during the etching process as depicted in Fig 9.

Pulse current anodization of porous silicon is applied by a sequence of current pulses. During the pause period of anodic current, H_2 bubbles will desorb. Desorption of the H_2 bubbles allows fresh HF species inside the pores to react with silicon wall that sustains the etching process at appreciable rate. This process will increase the thickness of the porous silicon layer thus, enhancing the porous layer intensity [61].

Experimental Procedures

- Porous silicon samples were prepared by electrochemical etching of p-type silicon, boron doped, and 0.75-1.25 Ω cm wafers.
- The electrolytic cell is described in.
- Aluminum film was deposited on the back side of the samples to improve the uniformity of the anodic current.
- The electrolyte solution was a mixture of hydrofluoric acid (HF 49%) and ethanol (95%), 1:4 by volume.
- Anodization process was carried out for 30 min for all samples.
- An output signal from a pulse current generator was used to feed the current through the anodic etching circuit.

Note that both the cycle time (T) and the pause time (T off) were adjusted.

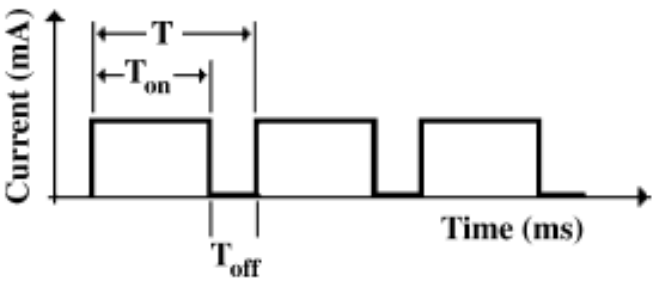

Figure 9. Schematic diagram of wave form of the pulse current used in the etching process [62] .

The PS formation sequence according to the current burst model is given as follows:

- Direct dissolution of silicon.
- Oxidization of silicon.
- Silicon oxide is dissolved.
- A slow surface passivation by H_2 starts at the clean surface.

To start the cycle again, each current burst has to overcome this H-passivation of the surface.

This process shows that there is significant freedom of choice available in peak spontaneous emission wavelength.

In this paper, we employ a novel and simple fabrication technique which employs Xenon Difluoride (XeF_2)-based dry isotropic etching to selectively form porous silicon in bulk single crystal silicon wafers [63]. XeF_2 is plasma-less etching technique and is based on the reaction of the fluorine ions, which represents the main etchant, with the solid silicon to produce – at room temperature – the volatile gas SiF_4. In a XeF_2-based etching process, a standard hard baked layer of photoresist can serve as a masking layer. In addition to its etching process simplicity, XeF_2 has a high etch selectivity to silicon. It reacts readily with silicon, but is relatively inert to photoresistance, silicon dioxide, silicon nitride and aluminum, which allows this technique to be used in the presence of CMOS integrated circuits as a post processing step. This is not the case when HF-based etching is used, as this latter will etch or damage the circuitry without a very hard mask followed by complex post-processing to remove the mask.

VI. METHODS

We utilized XeF_2 dry etching to create porous silicon surfaces on single crystalline silicon wafers. We used 3 inch diameter, 381± 20 μm thick <100> boron-doped (5–10 ohm cm) silicon wafers. The wafer was cut into 1.3 X 1.3 cm^2 that were then loaded in the XeF_2 etching chamber. The XeF_2 etching process does not depend on the silicon crystal orientation or its dopant content.

The fabrication process is achieved in a sequence of steps. First, undissociated gaseous XeF_2 is adsorbed onto the exposed areas of bulk silicon. The adsorbed gas is then dissociated into xenon and fluorine, after which the fluorine ions react with silicon to produce SiF_4 gas. Dissociation of the gas phase at room temperature leaves behind a porous

silicon surface. In this process, increasing the etching process time increases the overall size of the pores and the thickness of the porous silicon film. The chemical reaction for the etching of silicon by XeF_2 is: $Si + 2XeF_2 \rightarrow SiF_4 + 2Xe$. As a dry etching technique, there is no post-fabrication drying step required, thus reducing the risk of damage to the newly formed porous surface.

XeF_2 leaves behind porous silicon surfaces on top of the remaining bulk silicon with porous silicon layer thickness on the order of several hundreds of nanometers (600 to 700 nm). The obtained porosity depends on the etching time. Fig. 10 shows a representative Scanning Electron Microscope image of porous silicon sample prepared using XeF_2.

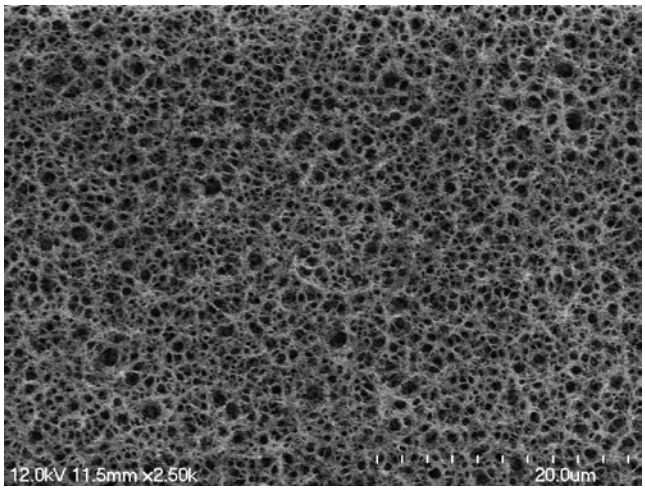

Figure 10. Scanning electron micrograph of a nanostructured porous silicon etched with XeF2.

VII. FABRICATION OF ENZYME ELECTRODES

The fabrication process of the comb capacitor starts with dicing 3 inch 381+20-mm-thick <100> boron doped (5–10 ohm-cm) silicon wafer into small 3x3 cm squared pieces. Metal layers of titanium (adhesion layer, 500 nm thick) and gold (conducting layer, 750 nm thick) were deposited by sputtering on the silicon wafer. A 1.4 micron thick layer of photoresist is then spun on and photolithographically patterned to define the inter-digitized fingers. The gold and titanium are then wet etched, with 1:2:10 I_2:KI:H_2O and 20:1:1 H_2O:HF:H_2O_2, respectively. Acetone was then used to remove the remaining photoresist thus exposing the gold layer covering the inter-digitized fingers. Fig. 11(a) is a scanning electron micrograph of the array of fingers. Fig. 11 (b) is a magnified view of the scanning electron microscope (SEM) picture of the network of pores fabricated selectively in between the silicon comb fingers covered with titanium-gold. Porous silicon layers with different porosities can be obtained by changing the etching recipes in the XeF2 system.

VIII. CONCLUSION AND FUTURE WORK

Nanostructured doped porous silicon is a promising material for Biofuel cells. It offers several advantages, including the use of silicon in microelectronics, biocompatibility, and simplicity in tailoring porosity and conductivity. Dry etching of porous silicon using XeF_2 allows, due to its compatibility with integrated circuits, allows an easy integration of porous silicon scaffolds with the microelectronic harvesting integrated circuit. Future work will focus on testing porous silicon samples in complete enzymatic fuel cell setup.

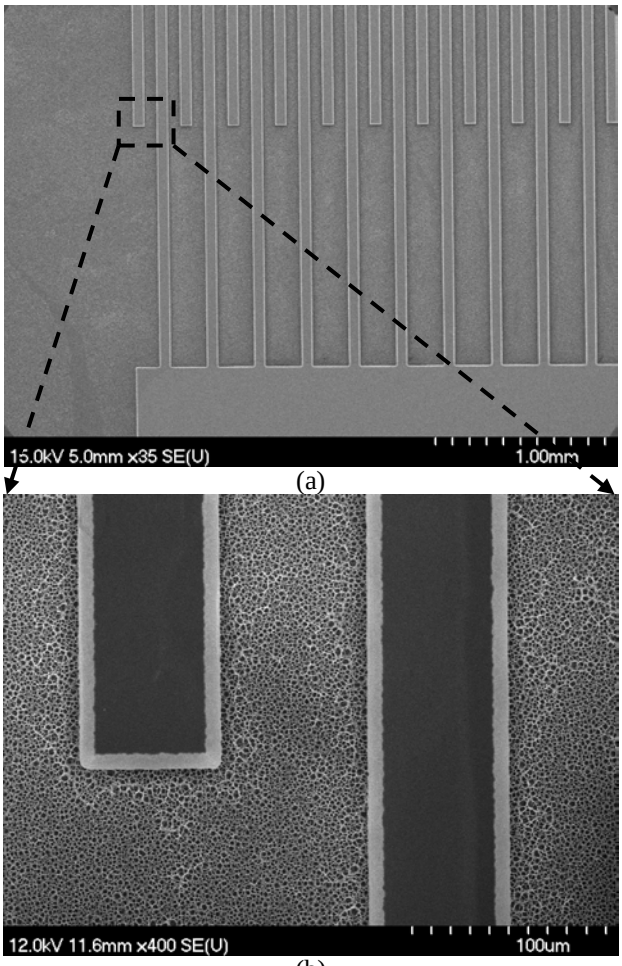

Figure 11. Scanning electron micrographs (a) novel inter-digitized energy harvesting electrodes (b) magnified view of two fingers with the porous area in between.

ACKNOWLEDGMENT

The current project is supported by the National Council for Scientific Research, Lebanon. The authors would like to acknowledge the assistance of the McGill's Nanotools and Microfabrication Laboratory, Montreal, in preparing the porous silicon samples, and the Lebanese International University for logistic assistance.

REFERENCES

[1] M. Hajj-Hassan, Hajj-Hassan, H., and H. M. Khachfe, "Nanostructured Porous Silicon Scaffolds for Biofuel Cells," The Second

International Conference on Global Health Challenges, Lisbon Portugal, pp. 38-42, 2013.

[2] P. D. Mitcheson, G. K. Rao, A. S. Holmes, and T. C. Green, "Energy Harvesting From Human and Machine Motion for Wireless Electronic Devices," Proceedings of the IEEE, vol. 96, pp. 1457-1486, 2008.

[3] S. Heydari Nasab, M. Asefi, L. Albasha, and N. Qaddoumi, "Investigation of RF Signal Energy Harvesting," Active and Passive Electronic Components, vol. 2010, 2010.

[4] H. Chun-Ching, S. An-Shen, and C. Jing-Chih, "Improvement of Pyroelectric Cells for Thermal Energy Harvesting," Sensors, pp. 534-548, 2012.

[5] N. G. Stephen, "On energy harvesting from ambient vibration," Journal of Sound and Vibration, vol. 293, pp. 409-425, 2006.

[6] H. A. Sodano, D. J. Inman, and G. Park, "Comparison of piezoelectric energy harvesting devices for recharging batteries," Journal of Intelligent Material Systems and Structures, vol. 16, pp. 799-807, 2005.

[7] S. P. Beeby, RN. Torah, MJ. Tudor, P. Glynne-Jones, T. O'Donnell, CR. Saha, and S. Roy, "A micro electromagnetic generator for vibration energy harvesting," Journal of Micromechanics and Microengineering, vol. 17, p. 1257, 2007.

[8] F. Cottone and H. Vocca, L. Gammaitoni, "Nonlinear energy harvesting, "Physical Review Letters, vol. 102, p. 080601, 2009.

[9] J. Q. Liu, H. B. Fang, Z. Y. Xu, X. H. Mao, X. C. Shen, H. Liao, and B. C. Cai, "A MEMS-based piezoelectric power generator array for vibration energy harvesting," Microelectronics Journal, vol. 39, pp. 802-806, 2008.

[10] H. B. Fang, Liu, J. Q., Xu, Z.Y., Dong, L., Wang, L., Chen, D., Cai, B.C., Liu, Y., "Fabrication and performance of MEMS-based piezoelectric power generator for vibration energy harvesting," Microelectronics Journal, vol. 37, pp. 1280-1284, 2006.

[11] J. A. Paradiso and T. Starner, "Energy scavenging for mobile and wireless electronics," Pervasive Computing, IEEE, vol. 4, pp. 18-27, 2005.

[12] H. Kulah and K. Najafi, "Energy scavenging from low-frequency vibrations by using frequency up-conversion for wireless sensor applications," Sensors Journal, IEEE, vol. 8, pp. 261-268, 2008.

[13] O. Zorlu, E. T. Topal, and H. Kulah, "A vibration-based electromagnetic energy harvester using mechanical frequency up-conversion method," Sensors Journal, IEEE, vol. 11, pp. 481-488, 2011.

[14] B. Jiang, J. R. Smith, M. Philipose, S. Roy, K. Sundara-Rajan, and A. V. Mamishev, "Energy scavenging for inductively coupled passive RFID systems," in Instrumentation and Measurement Technology Conference, 2005. IMTC 2005. Proceedings of the IEEE, 2005, pp. 984-989.

[15] M. Mi, M. H. Mickle, C. Capelli, and H. Swift, "RF energy harvesting with multiple antennas in the same space," Antennas and Propagation Magazine, IEEE, vol. 47, pp. 100-106, 2005.

[16] A. J. Stratakos, R. W. Brodersen, and S. R. Sanders, "High-efficiency low-voltage DC-DC conversion for portable applications," University of California, Berkeley, Fall 1998.

[17] A. T. Yahiro, S. M. Lee, and D. O. Kimble, "Bioelectrochemistry: I. Enzyme utilizing bio-fuel cell studies," Biochimica et Biophysica Acta (BBA)-Specialized Section on Biophysical Subjects, vol. 88, pp. 375-383, 1964.

[18] B. C. H. Steele and A. Heinzel, "Materials for fuel-cell technologies," Nature, vol. 414, pp. 345-352, 2001.

[19] R. Hahn, S. Wagner, A. Schmitz, and H. Reichl, "Development of a planar micro fuel cell with thin film and micro patterning technologies," Journal of Power Sources, vol. 131, pp. 73-78, 2004.

[20] T. J. Yen, N. Fang, X. Zhang, G. Q. Lu, and C.Y. Wang, "A micro methanol fuel cell operating at near room temperature," Applied Physics Letters, vol. 83, pp. 4056-4058, 2003.

[21] S. K. Chaudhuri and D. R. Lovley, "Electricity generation by direct oxidation of glucose in mediatorless microbial fuel cells," Nature biotechnology, vol. 21, pp. 1229-1232, 2003.

[22] B. E. Logan and J. M. Regan, "Microbial fuel cells-challenges and applications," Environmental science & technology, vol. 40, pp. 5172-5180, 2006.

[23] S. Calabrese Barton, J. Gallaway, and P. Atanassov, "Enzymatic biofuel cells for implantable and microscale devices," Chemical Reviews, vol. 104, pp. 4867-4886, 2004.

[24] B. E. Logan, B. Hamelers, R. Rozendal, U. Schröder, J. Keller, S. Freguia, P. Aelterman, W. Verstraete, and K. Rabaey, "Microbial fuel cells: methodology and technology," Environmental science & technology, vol. 40, pp. 5181-5192, 2006.

[25] Y. Han, C. Yu, and H. Liu, "A microbial fuel cell as power supply for implantable medical devices," Biosensors and Bioelectronics, vol. 25, pp. 2156-2160, 2010.

[26] I. A. Ieropoulos, J. Greenman, C. Melhuish, and J. Hart, "Comparative study of three types of microbial fuel cell," Enzyme and microbial technology, vol. 37, pp. 238-245, 2005.

[27] J. D. Keighron and C. D. Keating, "Enzyme: nanoparticle bioconjugates with two sequential enzymes: stoichiometry and activity of malate dehydrogenase and citrate synthase on Au nanoparticles," Langmuir, vol. 26, pp. 18992-19000, 2010.

[28] G. A. Justin, Y. Zhang, M. Sun, and R. Sclabassi, "An investigation of the ability of white blood cells to generate electricity in biofuel cells," in Bioengineering Conference, 2005. Proceedings of the IEEE 31st Annual Northeast, 2005, pp. 277-278.

[29] A. E. Franks and K. Nevin, "Microbial fuel cells, a current review," Energies, vol. 3, pp. 899-919, 2010.

[30] G. A. Justin, Y. Zhang, M. Sun, R. Sclabassi, "Biofuel cells: a possible power source for implantable electronic devices," in Engineering in Medicine and Biology Society, 2004. IEMBS'04. 26th Annual International Conference of the IEEE, 2004, pp. 4096-4099.

[31] P. Cinquin, C. Gondran, F. Giroud, S. Mazabrard, A. Pellissier, F. Boucher, J.P. Alcaraz, K. Gorgy, F. Lenouvel, and S. Mathé, "A glucose biofuel cell implanted in rats," PLoS One, vol. 5, p. e10476, 2010.

[32] S. C. Wang, F. Yang, M. Silva, A.W.Y. Zarow, and Z. Iqbal, "Membrane-less and mediator-free enzymatic biofuel cell using carbon nanotube/porous silicon electrodes," Electrochemistry Communications, vol. 11, pp. 34-37, 2009.

[33] C. Liu, S. Alwarappan, Z. Chen, X. Kong, and C.Z. Li, "Membraneless enzymatic biofuel cells based on graphene nanosheets," Biosensors and Bioelectronics, vol. 25, pp. 1829-1833, 2010.

[34] D. Schumacher, J. Vogel, and U. Lerche, "Construction and applications of an enzyme electrode for determination of galactose and galactose-containing saccharides," Biosensors and Bioelectronics, vol. 9, pp. 85-89, 1994.

[35] W. Sun, J.E. Puzas, T.J. Sheu, and P.M. Fauchet, "Porous silicon as a cell interface for bone tissue engineering," Physica Status Solidi A-Applications and Materials Science, vol. 204, pp. 1429-1433, 2007.

[36] M. Hajj-Hassan, M. Khayyat-Kholghi, H. Wang, V. Chodavarapu, and J.E. Henderson, "Response of murine bone marrow-derived mesenchymal stromal cells to dry-etched porous silicon scaffolds," J Biomed Mater Res Part A, pp. 269-274, 2011.

[37] S. Chan, P. M. Fauchet, Y. Li, L. J. Rothberg, and B. L. Miller, "Porous silicon microcavities for biosensing applications," Physica Status Solidi a-Applied Research, vol. 182, pp. 541-546, Nov 2000.

[38] R. A. Williams and H. W. Blanch, "Covalent Immobilization of Protein Monolayers for Biosensor Applications," Biosensors & Bioelectronics, vol. 9, pp. 159-167, 1994.

[39] A. Janshoff, K. P. S. Dancil, C. Steinem, D. P. Greiner, V. S. Y. Lin, C. Gurtner, K. Motesharei, M. J. Sailor, and M. R. Ghadiri, "Macroporous

p-type silicon Fabry-Perot layers. Fabrication, characterization, and applications in biosensing," Journal of the American Chemical Society, vol. 120, pp. 12108-12116, Nov 25 1998.

[40] J. L. Coffer, M. A. Whitehead, D. K. Nagesha, P. Mukherjee, G. Akkaraju, M. Totolici, R. S. Saffie, and L. T. Canham, "Porous silicon-based scaffolds for tissue engineering and other biomedical applications," Physica Status Solidi A-Applications and Materials Science, vol. 202, pp. 1451-1455, Jun 2005.

[41] E. J. Anglin, L. Y. Cheng, W. R. Freeman, and M. J. Sailor, "Porous silicon in drug delivery devices and materials," Advanced Drug Delivery Reviews, vol. 60, pp. 1266-1277, Aug 17 2008.

[42] G. Lammel, S. Schweizer, S. Schiesser, and P. Renaud, "Tunable optical filter of porous silicon as key component for a MEMS spectrometer," Journal of Microelectromechanical Systems, vol. 11, pp. 815-828, Dec 2002.

[43] M. G. Berger, M. Thonissen, R. Arensfischer, H. Munder, H. Luth, M. Arntzen, and W. Theiss, "Investigation and Design of Optical-Properties of Porosity Superlattices," Thin Solid Films, vol. 255, pp. 313-316, Jan 15 1995.

[44] C. C. Striemer, T. R. Gaborski, J. L. McGrath, and P. M. Fauchet, "Charge- and size-based separation of macromolecules using ultrathin silicon membranes," Nature, vol. 445, pp. 749-753, Feb 15 2007.

[45] H. Foll, M. Christophersen, J. Carstensen, and G. Hasse, "Formation and application of porous silicon," Materials Science & Engineering R-Reports, vol. 39, pp. 93-141, Nov 1 2002.

[46] E. A. de Vasconcelos, E.F. da Silva, B.D. Santos, W.M. de Azevedo, and J.A.K. Freire, "A new method for luminescent porous silicon formation: reaction-induced vaporphase stain etch," Phys. Status Solidi A—Appl. Mat, vol. 202, pp. 1539–1542, 2005.

[47] R. L. Smith and S. D. Collins, "Porous Silicon Formation Mechanisms," Journal of Applied Physics, vol. 71, pp. R1-R22, Apr 15 1992.

[48] J. Escorcia-Garcia, O. Sarracino Martínez, J. M. Gracia-Jiménez, and V. Agarwal, "Porous silicon photonic devices using pulsed anodic etching of lightly doped silicon," Journal of Physics D: Applied, vol. 42, p. 145101 (7pp), 2009.

[49] T. Nakagawa, H. Koyama, and N. Koshida, "Control of structure and optical anisotropy in porous Si by magnetic-field assisted anodization," Applied Physics Letters, vol. 69, pp. 3206-3208, Nov 18 1996.

[50] Z. C. Feng and R. Tsu, Porous Silicon: World Scientific Pub Co Inc, 1994.

[51] M. Bouchaour, A. Ould-Abbas, N. Diaf, and N.C. Sari, "Effect of drying on porous silicon," J Therm Anal Calorim, vol. 76, pp. 677–684, 2004.

[52] S. Boughaba and K. Wang, "Fabrication of porous silicon using a gas etching method," Thin Solid Films, vol. 497, pp. 83-89, 2006.

[53] J. Xu and A. J. Steckl, "Stain ‐ etched porous silicon visible light emitting diodes," Journal of Vacuum Science & Technology B, vol. 13, pp. 1221-1224, 1995.

[54] A. Hidekazu, M. Akira, K. Akira, A. Tomoyoshi, and S. Akinobu, "A Comparative Study of Visible Photoluminescence from Anodized and from Chemically Stained Silicon Wafers," Japanese Journal of Applied Physics, vol. 32, p. L1, 1993.

[55] M. T. Kelly, J. Chun, K. M. Bocarsly, and B. Andrew, "High efficiency chemical etchant for the formation of luminescent porous silicon," Applied Physics Letters, vol. 64, pp. 1693-1695, 1994.

[56] V. Lehmann, H and Föll, "Formation Mechanism and Properties of Electrochemically Etched Trenches in n-Type Silicon," J. Electrochem. Soc. , vol. 137, pp. 653-659, 1990.

[57] S. Shih, K. H. Jung, T. Y. Hsieh, J. Sarathy, J. C. Campbell, and D. L. Kwong, "Photoluminescence and formation mechanism of chemically etched silicon," Applied Physics Letters, vol. 60, pp. 1863-1865, 1992.

[58] Y. Naokatsu and T. Hiroshi, "Blue Luminescence from Photochemically Etched Silicon," Japanese Journal of Applied Physics, vol. 38, p. 5706, 1999.

[59] N. Yamamoto and H. Takai, "Formation mechanism of silicon based luminescence material using a photo chemical etching method," Thin Solid Films, vol. 388, pp. 138-142, 2001.

[60] A. M. Hynes, H. Ashraf, J. K. Bhardwaj, J. Hopkins, I. Johnston, and J. N. Shepherd, "Recent advances in silicon etching for MEMS using the ASE™ process," Sensors and Actuators A: Physical, vol. 74, pp. 13-17, 1999.

[61] A. A. Aziz, "Fabrication and characterization of uniform quantum size porous silicon," Materials science forum, vol. 517, pp. 232-236, 2006.

[62] N. K. Ali, M. R. Hashim, A. Abdul Aziz, I. Hamammu, "Method of controlling spontaneous emission from porous silicon fabricated using pulsed current etching," Solid-State Electronics, vol. 52, pp. 249-254, 2008.

[63] M. Hajj-Hassan, M. Cheung, and V. Chodavarapu, "Dry etch fabrication of porous silicon using xenon difluoride," Micro & Nano Letters, IET, vol. 5, pp. 63-69, 2010.